



**HAL**  
open science

## Mid-infrared spectroscopy to trace biogeochemical changes of earthworm casts during ageing under field conditions

N. Bottinelli, P. Jouquet, T.M. Tran, H. Aroui Boukbida, C. Rumpel

► **To cite this version:**

N. Bottinelli, P. Jouquet, T.M. Tran, H. Aroui Boukbida, C. Rumpel. Mid-infrared spectroscopy to trace biogeochemical changes of earthworm casts during ageing under field conditions. *Geoderma*, 2021, 383, pp.114811. 10.1016/j.geoderma.2020.114811 . hal-03492660

**HAL Id: hal-03492660**

**<https://hal.science/hal-03492660>**

Submitted on 7 Nov 2022

**HAL** is a multi-disciplinary open access archive for the deposit and dissemination of scientific research documents, whether they are published or not. The documents may come from teaching and research institutions in France or abroad, or from public or private research centers.

L'archive ouverte pluridisciplinaire **HAL**, est destinée au dépôt et à la diffusion de documents scientifiques de niveau recherche, publiés ou non, émanant des établissements d'enseignement et de recherche français ou étrangers, des laboratoires publics ou privés.



Distributed under a Creative Commons Attribution - NonCommercial 4.0 International License

1 **Mid-infrared spectroscopy to trace biogeochemical changes of earthworm casts during**  
2 **ageing under field conditions**

3

4 N. Bottinelli<sup>1,2</sup>; P. Jouquet<sup>2</sup>; T.M. Tran<sup>1</sup>, H. Aroui Boukbida<sup>2</sup>; C. Rumpel<sup>2</sup>

5 <sup>1</sup> Soils and Fertilizers Research Institute (SFRI), Duc Thang, Bac Tu Liem, Hanoi, Vietnam

6 <sup>2</sup>IRD, CNRS, Institut d'écologie et des sciences de l'environnement (IESS-Paris UMR

7 Sorbonne Université, UPEC, CNRS, IRD, INRAe), FEST team, F-93143 Bondy, France

8

9 corresponding author : Nicolas Bottinelli (email : [nicolas.bottinelli@ird.fr](mailto:nicolas.bottinelli@ird.fr))

10

11

12 **Abstract**

13 Earthworm cast ageing controls soil ecosystem services such as carbon storage and nutrient  
14 availability. To test the hypothesis that biogeochemical changes during casts ageing can be  
15 traced by infrared spectroscopy, we collected topsoil aggregates and earthworm casts  
16 produced by the anecic earthworm *Amyntas khami* belonging to five distinct degradation  
17 stages in woodland in northern Vietnam. We analysed mid-infrared (MIR) spectra of both  
18 sample types using two approaches: (1) calculation of the proportion of aliphatic compounds  
19 and the humification index of organic matter (OM) using specific wavenumbers and (2) linear  
20 discriminant analysis (LDA) of the most important peaks and shoulders of the entire  
21 spectrum. Our results showed that aliphatic compound contribution to OM was similar and  
22 the humification index of OM lower (2-fold) in casts as compared to topsoil aggregates  
23 independent of their degradation stage. In contrast, LDA showed a continuous shift from fresh  
24 casts to aged casts and topsoil aggregates in agreement with biogeochemical changes of cast  
25 properties. We thus conclude that MIR analysis of bulk samples and LDA taking into account  
26 the absorbance intensity of most important wavenumbers is a promising tool to capture  
27 biogeochemical alterations of organic and mineral earthworm cast properties during ageing.

28

29 **Key words:** bioturbation; aggregation; macrofauna; FTIR spectroscopy

30

31

32

33

34

35

36

## 37 **Introduction**

38 Earthworms impact soil properties through their activity. In particular, they have a strong  
39 influence on soil organic matter (OM) storage and chemical composition through cast  
40 formation, which leads to enrichment of particulate OM occluded in aggregates (Bossuyt et  
41 al., 2004) and association of OM with minerals (Barthod et al., 2020). It was shown that the  
42 elemental content (Decaëns et al., 1999), and the composition of OM undergo changes after  
43 cast deposition. These changes reflect different cast ageing stages, which have distinct  
44 biogeochemical properties compared to surrounding soil aggregates without earthworm  
45 influence (Bottinelli et al., 2020). In the present study, we used mid infrared spectroscopy  
46 (MIR) to generate spectral fingerprints, which may allow in combination with chemometric  
47 approaches for the differentiation of cast degradation stages and topsoil aggregates. This  
48 technique has the advantage of being inexpensive and rapid. It has already been used to assess  
49 the biogenic origin of soil aggregates (Jouquet et al., 2009), and to identify biostructures  
50 produced by earthworms and their age (Dominguez-Haydar et al., 2020; Zangerlé et al.,  
51 2014). However, up to date, this method has never been used to follow biogeochemical  
52 changes of cast properties during field ageing. In this study we aimed to differentiate five  
53 different degradation stages of casts produced by the anecic earthworm *Amyntas khami* using  
54 mid-infrared (MIR) spectroscopy and two different approaches of data exploitation. We  
55 hypothesised that changes in organic compounds during the degradation of casts would be  
56 captured by MIR spectroscopy.

57 We sampled earthworm casts produced by the anecic earthworm species *A. khami* and  
58 topsoil aggregates in subtropical woodland in northern Vietnam (20° 57'N, 105° 29'E) in close  
59 proximity at sampling locations with similar microclimatic conditions. The soil type was  
60 Acrisol (WRB) (Podwojewski et al., 2008), with an organic carbon content of 2.5%, a clay  
61 content of 50% and a pH (H<sub>2</sub>O) of 5. The mass of casts found at the time of sampling

62 represented 4400 g (oven dry weight) per m<sup>2</sup>. We collected five replicates of casts with  
63 different degradation stages (A to E) differentiated by visual aspects and adjacent topsoil (2–7  
64 cm depth) without visible earthworm activity. Cast A and B were fresh humid casts assumed  
65 to be 1 day and 1 week old. Cast C was in dry state. D casts showed signs of degradation  
66 (greenish colour due to the presence algae with cracks at the surface). The size of casts (A to  
67 D) and topsoil aggregates varied from 5 to 15 cm. Casts were produced through the  
68 accumulation of fecal pellets deposited the one on the other. After disintegration probably due  
69 to livestock trampling, human traffic, root growth and raindrop impact or natural aggregate  
70 turnover, individual pellet of 1 cm diameter were released: cast E of unknown age, consisting  
71 of small aggregates and representing the last stage of degradation recognizable by naked eye.  
72 MIR spectra of air-dry ground samples (< 200 µm) were collected with a Fourier Transform  
73 Spectrophotometer (FTIR 660 Agilent ex-Varian, Agilent Technologies, Inc., Santa Clara,  
74 USA), operating in diffuse reflectance mode. Measurements were made at 2 cm<sup>-1</sup> intervals in  
75 the MIR range (4000-400 cm<sup>-1</sup>) and converted to absorbance. The raw spectra were subjected  
76 to pre-processing, including Savitzky-Golay smoothing (first order polynomial filter with a  
77 13-point window), baseline correction (polynomial fitting with degree 3) and normalisation  
78 by the sum of absorbance across 4,000-400 cm<sup>-1</sup>.

79 The MIR spectra of earthworm casts and soil aggregates featured common peaks,  
80 with relatively similar intensities (**Fig. S1**). At first, we assessed OM changes during  
81 earthworm cast ageing through calculation of aliphatic compound contribution and the  
82 humification index (Demyan et al., 2012; Margenot and Odson, 2016). In fact, the digestion  
83 of fresh OM by anecic species and microbial activity in casts might result in degradation of  
84 easily decomposable OM compounds and concomitant increase of aliphatic and aromatic OM  
85 compounds and the humification index (Barthod et al., 2020). Aliphatic compound  
86 contribution was calculated as the absorbance intensity of C-H signals at 3010-2810 cm<sup>-1</sup>

87 determined from the tangential baseline and normalized with the soils' organic carbon  
88 content. In addition, the humification index was computed as the ratio of aliphatic absorbance  
89 intensity with the absorbance intensity of aromatic C=C, ketone and quinone C=O, and/or  
90 amide C=O at 1660-1580  $\text{cm}^{-1}$  determined from the total baseline. One-way ANOVA was  
91 used to compare these two indicators of OM changes in casts of different degradation stages  
92 and topsoil aggregates ( $n = 5$ ). Prior to running ANOVA, the data were tested for  
93 homogeneity of variances and normality and log-transformed when required. LSD post hoc  
94 multiple comparison tests were used when the effects were significant. Differences among  
95 treatments were declared significant at the 0.05 probability level. ANOVA and LSD tests  
96 were performed with "car" and "agricolae" packages of the R software. Our data showed that  
97 the aliphatic peak intensity was greater in casts compared with topsoil aggregates without  
98 difference among different degradation stages (**Fig. 1a**). The aliphatic peak intensity  
99 normalized by soil organic carbon was similar in all samples (**Fig. 1b**). The humification  
100 index of OM was smaller in casts than topsoil aggregates without difference among cast  
101 degradation stages (**Fig. 1c**). Our results thus showed that direct interpretation of MIR signals  
102 with general indicators assigned to OM compounds in an ANOVA did not distinguish cast  
103 degradation stages. They were somehow useful to differentiate earthworm casts from topsoil  
104 aggregates, containing less fresh OM (Guggenberger et al., 1996).

105 Our second strategy to differentiate earthworm cast degradation stages was based on  
106 linear discriminant analysis (LDA) of important peaks and shoulders of the MIR spectra.  
107 These signals were identified using the software OriginPro and the local maximum method  
108 (local points equal 5): 2 peaks (3616 and 3427) from the region 4000-2800  $\text{cm}^{-1}$  and 13 peaks  
109 (1942, 1874, 1622, 1595, 1527, 1456, 1275, 1163, 1109, 1009, 949, 823, 708  $\text{cm}^{-1}$ ) from the  
110 region 2000 to 600  $\text{cm}^{-1}$  using the total baseline and (ii) 2 peaks (2920 and 2850  $\text{cm}^{-1}$ ) from  
111 the region 3010-2810  $\text{cm}^{-1}$  using the tangential baseline (**Fig. S1**).

112 LDA is a multivariate supervised technique that maximizes the ratio of the between group  
113 variance to the within group variance. The Pillai test was used to verify the statistical  
114 significance of the discrimination. Our data showed that LDA was able to differentiate the  
115 five types of casts and the topsoil aggregates ( $p < 0.05$ , Pillai test) (**Fig. 2**). The first axis  
116 explaining 30% of the variability, differentiated cast A-E from topsoil aggregates reflecting  
117 their gradually changing properties (Bottinelli et al., 2020). The first axis was correlated to  
118 3427, 2850, 2925, 1622, 1595, and 1456  $\text{cm}^{-1}$  in the negative direction and 1942  $\text{cm}^{-1}$  in the  
119 positive direction. Intensities of these wavenumbers may be related to OM as well as mineral  
120 soil constituents (Parikh et al., 2014). In particular, the band at 3400  $\text{cm}^{-1}$  was found to be  
121 correlated with contribution of the light fraction to whole soil (Calderón et al., 2011). Light  
122 fractions are generally composed of fresh plant litter and were reported as early indicators of  
123 OM changes (Leifeld and Kögel-Knabner, 2005). The wavenumbers 1595 and 1456  $\text{cm}^{-1}$  may  
124 be related to amide and carboxylate C, which are typical OM compounds subjected to change  
125 during OM degradation (Parikh et al., 2014). The wavenumber 1942  $\text{cm}^{-1}$  corresponds to  
126 quartz and its gradual increase in intensity from cast A to topsoil aggregates might suggest the  
127 preferential loss of mineral constituents caused by rainfall (Nooren et al., 1995). Degradation  
128 of OM occurring during cast ageing and change in mineral composition thus explained the  
129 differentiation of the samples along axis 1. The second axis (explaining 25% of the  
130 variability) differentiated cast C, which showed lower absorbance intensity at 3616  $\text{cm}^{-1}$  as  
131 compared to other casts and topsoil aggregates. Since this wavenumber corresponds to  
132 kaolinite, biogeochemical changes occurring at this stage may again involve mineral cast  
133 constituents. The heatmap (**Fig. S2**) based on the correlation matrix of significant peak  
134 intensities of MIR spectra (**Fig. 2**) with soil OM properties measured by Bottinelli et al.  
135 (2020) separated two groups of wavenumbers: (i) 3427, 2850, 1595 and 2925, 1622 and 1456  
136  $\text{cm}^{-1}$  and (ii) 3616 and 1942  $\text{cm}^{-1}$ . The first group was positively related to organic C

137 characteristics, while the second group may be related to involvement of mineral compounds  
138 in cast ageing because of its negative correlation with organic C. Our results therefore showed  
139 that MIR spectroscopy combined with multivariate analysis is capable of separating casts  
140 according to their degradation stage. Similar results were obtained by Zangerlé et al. (2014)  
141 and Dominguez-Haydar et al. (2020), who used near infrared spectroscopy to discriminate casts  
142 of different ages produced by lumbricid species in the laboratory. Contrary to Zangerlé et al.  
143 (2014), we found that field ageing affects not only organic but also mineral compounds  
144 possibly through selective loss of particles or soluble compounds.

145 We thus conclude that MIR analysis of bulk samples and LDA taking into account the  
146 absorbance intensity of the most important wavenumbers contributing to cast spectra is  
147 capable of capturing biogeochemical changes occurring during ageing and degradation of  
148 earthworm casts in the field.

149

## 150 **Acknowledgements**

151 This study was financially supported by CNRS/INSU (VINAWORM research project) under  
152 the framework of the EC2CO program. We acknowledge the technical assistance of the  
153 farmers in Dong Cao village, as well as L. Ganesha for his unconditional support. Data from  
154 this study were partially obtained from the ALYSES facility (IRD-UPMC) which was  
155 supported by grants from Région Ile de France. Dong Cao is part of Multiscale Tropical  
156 Catchments (M-Tropics) project (<https://mtropics.obs-mip.fr/>) supported by the French  
157 Institute of Research for Development (IRD).

158

159

## 160 **References**

161 Barthod, J., Dignac, M.-F., Mer, G. Le, Bottinelli, N., Watteau, F., Kögel-Knabner, I.,



162 Rumpel, C., 2020. How do earthworms affect organic matter decomposition in the  
163 presence of clay-sized minerals? *Soil Biol. Biochem.* 107730.  
164 [https://doi.org/https://doi.org/10.1016/j.soilbio.2020.107730](https://doi.org/10.1016/j.soilbio.2020.107730)

165 Bossuyt, H., Six, J., Hendrix, P.F., 2004. Rapid incorporation of carbon from fresh residues  
166 into newly formed stable microaggregates within earthworm casts. *Eur. J. Soil Sci.* 55,  
167 393–399. <https://doi.org/10.1111/j.1351-0754.2004.00603.x>

168 Bottinelli, N., Kaupenjohann, M., Märten, M., Jouquet, P., Soucémarianadin, L., Baudin, F.,  
169 Minh, T.T., Rumpel, C., 2020. Age matters: Fate of soil organic matter during ageing of  
170 earthworm casts produced by the anecic earthworm *Amyntas khami*. *Soil Biol.*  
171 *Biochem.* 107906.

172 Calderón, F.J., Reeves, J.B., Collins, H.P., Paul, E.A., 2011. Chemical differences in soil  
173 organic matter fractions determined by diffuse-reflectance mid-infrared spectroscopy.  
174 *Soil Sci. Soc. Am. J.* 75, 568–579.

175 Decaëns, T., Rangel, A.F., Asakawa, N., Thomas, R.J., 1999. Carbon and nitrogen dynamics  
176 in ageing earthworm casts in grasslands of the eastern plains of Colombia. *Biol. Fertil.*  
177 *Soils* 30, 20–28. <https://doi.org/10.1007/s003740050582>

178 Demyan, M.S., Rasche, F., Schulz, E., Breulmann, M., Müller, T., Cadisch, G., 2012. Use of  
179 specific peaks obtained by diffuse reflectance Fourier transform mid-infrared  
180 spectroscopy to study the composition of organic matter in a Haplic Chernozem. *Eur. J.*  
181 *Soil Sci.* 63, 189–199.

182 Dominguez-Haydar, Y., Velásquez, E., Zangerlé, A., Lavelle, P., Gutiérrez-Eisman, S.,  
183 Jiménez, J.J., 2020. Unveiling the age and origin of biogenic aggregates produced by  
184 earthworm species with their NIRS fingerprint in a subalpine meadow of Central  
185 Pyrenees. *PLoS One* 15, e0237115.

186 Jouquet, P., Zangerle, A., Rumpel, C., Brunet, D., Bottinelli, N., Tran Duc, T., 2009.

187 Relevance and limitations of biogenic and physicogenic classification: A comparison of  
188 approaches for differentiating the origin of soil aggregates. *Eur. J. Soil Sci.* 60, 1117–  
189 1125. <https://doi.org/10.1111/j.1365-2389.2009.01168.x>

190 Leifeld, J., Kögel-Knabner, I., 2005. Soil organic matter fractions as early indicators for  
191 carbon stock changes under different land-use? *Geoderma* 124, 143–155.

192 Margenot, A.J., Odson, A.K., 2016. Relationships between labile soil organic matter and  
193 nematode communities Relationships between labile soil organic matter and nematode  
194 communities in a California oak woodland. *Nematology* 18, 1231–1245.  
195 <https://doi.org/10.1163/15685411-00003027>

196 Nooren, C.A.M., van Breemen, N., Stoorvogel, J.J., Jongmans, A.G., 1995. The role of  
197 earthworms in the formation of sandy surface soils in a tropical forest in Ivory Coast.  
198 *Geoderma* 65, 135–148. [https://doi.org/10.1016/0016-7061\(94\)00035-9](https://doi.org/10.1016/0016-7061(94)00035-9)

199 Parikh, S.J., Goyne, K.W., Margenot, A.J., Mukome, F.N.D., Calderón, F.J., 2014. Soil  
200 chemical insights provided through vibrational spectroscopy, in: *Advances in*  
201 *Agronomy*. Elsevier, pp. 1–148. <https://doi.org/10.1016/B978-0-12-800132-5.00001-8>

202 Podwojewski, P., Orange, D., Jouquet, P., Valentin, C., Nguyen, V.T., Janeau, J.L., Tran,  
203 D.T., 2008. Land-use impacts on surface runoff and soil detachment within agricultural  
204 sloping lands in Northern Vietnam. *Catena* 74, 109–118.  
205 <https://doi.org/10.1016/j.catena.2008.03.013>

206 Zangerlé, A., Hissler, C., Blouin, M., Lavelle, P., 2014. Near infrared spectroscopy (NIRS) to  
207 estimate earthworm cast age. *Soil Biol. Biochem.* 70, 47–53.  
208 <https://doi.org/10.1016/j.soilbio.2013.11.023>

209

210 **Figure captions**

211 **Figure S1:** Average of MIR spectra showing mineral and organic peaks from earthworm casts  
212 presenting different degradation stages (A to E) and topsoil aggregates presenting no recent  
213 earthworm activity (n= 5). All spectra were smoothed, baseline corrected and normalized.

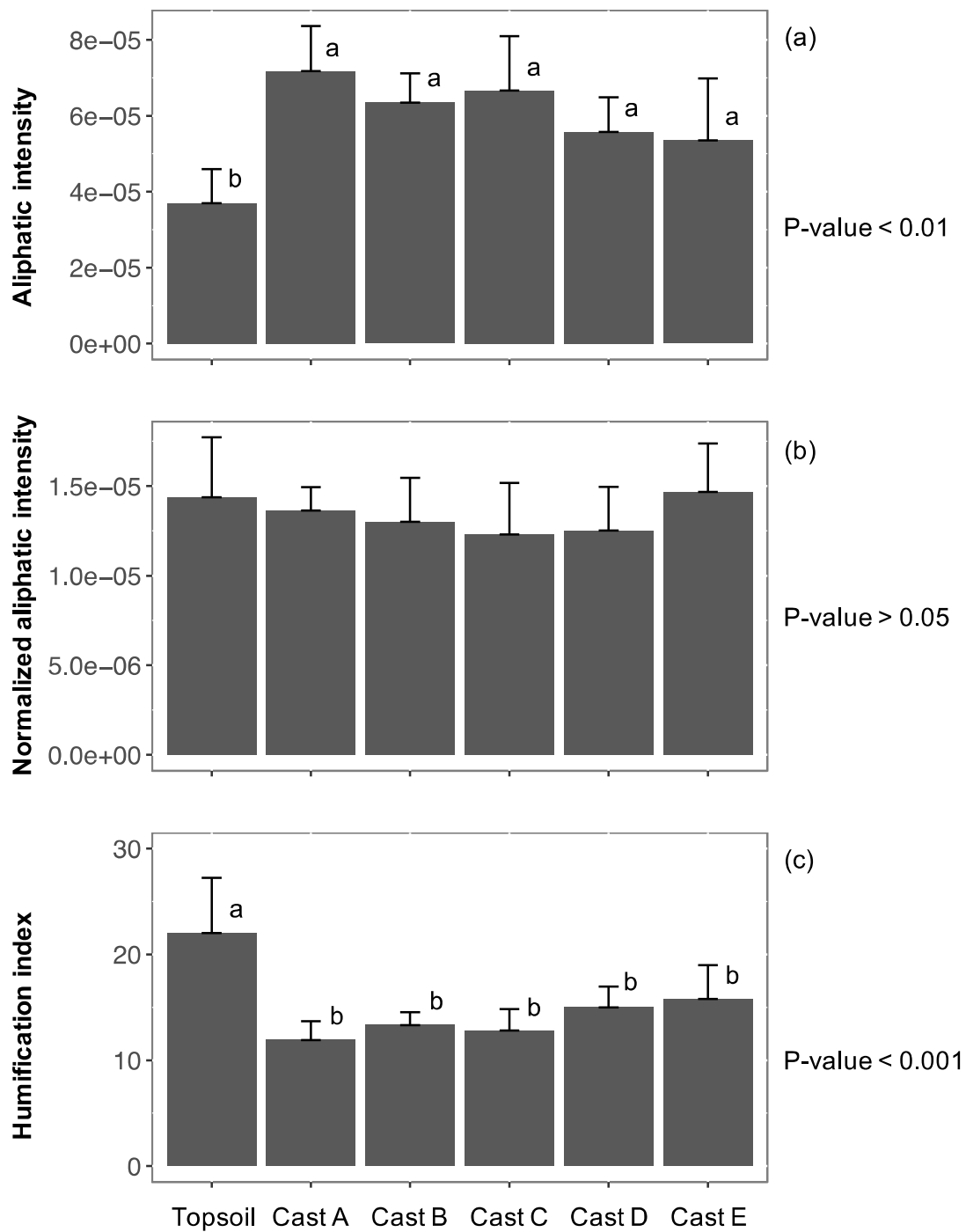
214 **Figure 1:** Average values (n = 5) of MIR peak intensity of C-H vibration from aliphatic  
215 carbon at 3010-2800 cm<sup>-1</sup> (a), aliphatic carbon normalised by soil carbon (b) and humification  
216 index (c) for earthworm casts presenting different degradation stages and topsoil aggregates.  
217 Error bars indicate standard errors and letters denote statistical differences across samples.

218 **Figure 2:** LDA showing the differentiation of earthworm cast presenting different  
219 degradation stages (A to E) and topsoil aggregates based on the 17 peaks found on MIR  
220 spectra (**Fig. S1**). Ellipses correspond to 67 % confidence intervals around the species  
221 barycenter. The most important peaks contributing to the discrimination of the group samples  
222 (cosines between the wavenumbers and the canonical scores > 0.35 or < -0.35) are colored in  
223 red.

224 **Figure S2:** Heatmap based on the correlation matrix of significant peak intensities found on  
225 MIR spectra (Fig. 1) with soil OM properties measured in Bottinelli et al. (Bottinelli et al.,  
226 2020) for earthworm casts presenting different degradation stages (A to E) and topsoil  
227 aggregates presenting no recent earthworm activity. OM properties are percentage of lignin,  
228 N-containing, polysaccharides and unspecific compounds measured by pyrolysis; OC content  
229 and C/N ratio of the whole aggregate and OC the three physical fractions (macro-aggregate  
230 (mac.), micro-aggregates (mic.) and mineral-associated (min.)). Peaks are sorted according to  
231 a cluster analysis. Green color indicates positive correlations, red color indicates negative  
232 correlations and the strength of color indicates the magnitude of correlation coefficient, as  
233 shown on the correlation spectrum (inset top right).

234

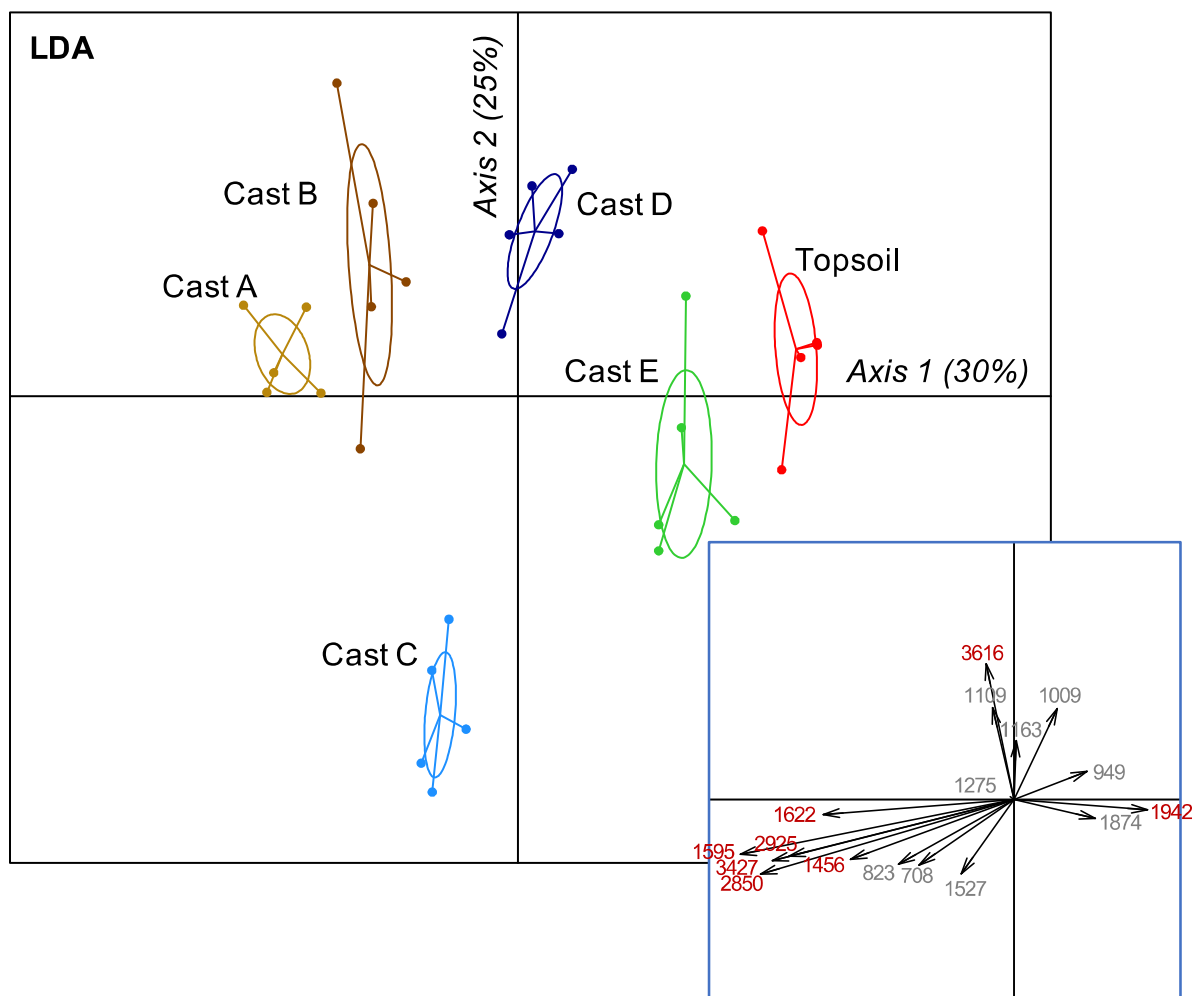
235



236

237 **Fig. 1:** Average values (n = 5) of MIR peak intensity of C-H vibration from aliphatic carbon  
 238 at 3010-2800 cm<sup>-1</sup> (a), aliphatic carbon normalised by soil carbon (b) and humification index  
 239 (c) for earthworm casts presenting different degradation stages and topsoil aggregates. Error  
 240 bars indicate standard errors and letters denote statistical differences across samples.

241



242

243 **Fig. 2:** LDA showing the differentiation of earthworm cast presenting different degradation

244 stages (A to E) and topsoil aggregates based on the 17 peaks found on MIR spectra (**Fig. S1**).

245 Ellipses correspond to 67 % confidence intervals around the species barycenter. The most

246 important peaks contributing to the discrimination of the group samples (cosines between the

247 wavenumbers and the canonical scores  $> 0.35$  or  $< -0.35$ ) are colored in red.

248

249

250